Preprint
UCRL-JC-139619

The Effect of Thermal Annealing and Second Harmonic Generation on Bulk Damage Performance of Rapid-Growth KDP Type I Doublers at 1064 nm

M. Runkel, S. Maricle, R. Torres, J. Auerbach, R. Floyd, R. Hawley-Fedder, A. K. Burnham

U.S. Department of Energy

Lawrence
Livermore
National
Laboratory

This article was submitted to
32nd Annual Symposium on Optical Materials for High Power Lasers
Boulder, CO
October 16-18, 2000

December 11, 2000

The effect of thermal annealing and second harmonic generation on bulk damage performance of rapid-growth KDP type I doublers at 1064 nm

Mike Runkel*, Stephen Maricle, Rich Torres, Jerry Auerbach, Randy Floyd, Ruth Hawley-Fedder and Alan K. Burnham

Lawrence Livermore National Laboratory, L-250, Livermore CA 94550

ABSTRACT

This paper discusses the results of thermal annealing and in-situ second harmonic generation (SHG) damage tests performed on six rapid growth KDP type 1 doubler crystals at 1064 nm (1ω) on the Zeus automated damage test facility. Unconditioned (S/1) and conditioned (R/1) damage probability tests were performed before and after thermal annealing, then with and without SHG on six doubler crystals from the NIF-size, rapid growth KDP boule F6.

The tests revealed that unannealed, last-grown material from the boule in either prismatic or pyramidal sectors exhibited the highest damage curves. After thermal annealing at 160°C for seven days, the prismatic sector samples increased in performance ranging from 1.6 to 2.4X, while material from the pyramidal sector increased only modestly, ranging from 1.0 to 1.4X.

Second harmonic generation decreased the damage fluence by an average of 20 percent for the S/1 tests and 40 percent for R/1 tests. Conversion efficiencies under test conditions were measured to be 20 to 30 percent and compared quite well to predicted behavior, as modeled by LLNL frequency conversion computer codes.

The damage probabilities at the 1ω NIF redline fluence (scaled to 10 ns via $t^{0.5}$) for S/1 tests for the unannealed samples ranged from 20 percent in one sample to 90-100 percent for the other 5 samples. Thermal annealing reduced the damage probabilities to less than 35 percent for 3 of the poor-performing crystals, while two pyramidal samples remained in the 80 to 90 percent range. Second harmonic generation in the annealed crystal increased the S/1 damage probabilities on all the crystals and ranged from 40 to 100 percent.

In contrast, R/1 testing of an unannealed crystal resulted in a damage probability at the NIF redline fluence of 16%. Annealing increased the damage performance to the extent that all test sites survived NIF redline fluences without damage. Second harmonic generation in the R/1 test yielded a damage probability of less than 2 percent for the annealed crystal.

These results indicate that a combination of thermal and laser conditioning would virtually eliminate bulk damage at the highest NIF fluences and indicate the need for laser conditioning of NIF SHG crystals.

Keywords: KDP, laser damage, thermal annealing, laser conditioning, damage probability, second harmonic generation

1. INTRODUCTION

This series of experiments was performed to determine the damage performance of a current NIF-sized, rapid growth KDP doubler boule. This was necessary because the available data on thermal annealing and damage for rapid growth KDP crystals is limited to a few small boules and only one large boule (RG7B)[1]. The typical increase in damage performance due to thermal annealing, as defined by the shift in the 50% damage probability fluence, was approximately 20% for those tests. Since that time numerous refinements in the crystal growth process have been implemented, yielding larger, more consistent crystals, hopefully with higher damage resistance. Previous test samples were most often z-plates (to speed fabrication); however, we now know that different crystal cuts can exhibit substantially different damage behavior, as in the case of z vs.

THG cuts at 3ω [2]. Testing at 3ω has shown that late-growth samples can exhibit higher damage resistance than early growth although data exhibiting this effect is limited. Also, forensics performed on the rapid growth SHG crystal RG8B from the second high damage threshold (HDT2) campaign on Beamlet showed unexpected levels of bulk damage. In the last year we have placed stronger emphasis on the unconditioned S/1 test as an indicator of initial NIF performance in the absence of off-line laser conditioning. The R/1 test represents optimal laser conditioning that cannot be achieved on-line with NIF. These considerations demonstrated the need for a series of tests at 1ω to assess the current state-of-the-art for rapid growth KDP crystals.

To address these questions on a state-of-the-art crystal, six Type-I doubler cut samples were obtained from boule F6. As shown in Figure 1, the samples spanned the growth history of the boule in both the prism and pyramidal sectors. Samples F6-1 through F6-3 were exclusively pyramidal material with F6-3, F6-2 and F6-1 corresponding to early, middle and late growth respectively. Samples F6-5 and F6-6 were exclusively prismatic material while F6-4 was taken over the seed and contained both sectors but was mainly prismatic. For the prismatic samples F6-4 was early growth while F6-5 and F6-6 were middle and late growth material. The growth parameters of the boule were characterized as "typical" for current crystals. The solution was prepared and resaturated with salt containing residual EDTA (an iron complexing agent) that is used to reduce iron content during salt manufacture. All sample surfaces were finished by diamond turning but were left uncoated.

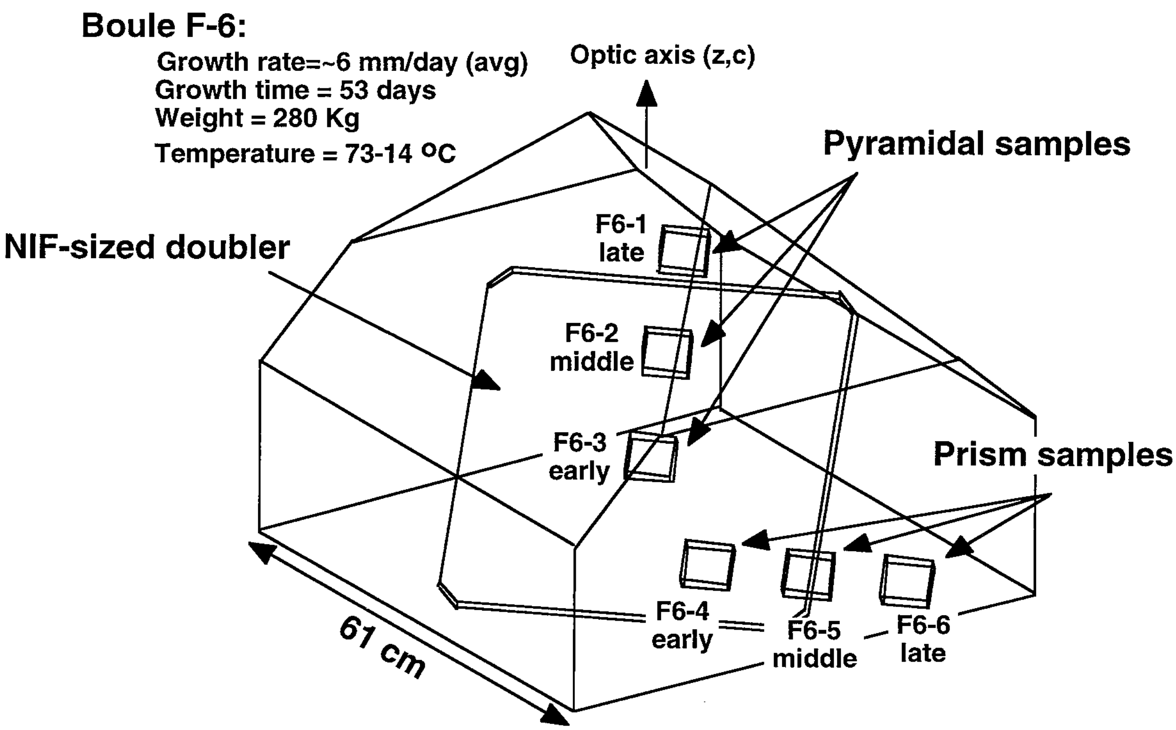

Figure 1. Side view schematic of F6 showing the location of doubler test samples. F6-1 through F6-3 are pyramidal material (late, middle and early growth respectively). F6-5 and F6-6 are middle and late growth prismatic material and F6-4 represents early growth prismatic material.

The damage tests performed on the samples consisted of the standard S/1 and R/1 damage probability tests using the Zeus damage test facility. The S/1 test consists of exposing a minimum of 10 test sites per fluence and measuring the number that damage. The fluence is then changed to measure damage probabilities covering the range from zero to 100 percent. In this way the damage probability curve as a function of fluence can be built up. Each test typically takes on the order of 60-100 individual test sites. The R/1 test consists of exposing each site to a ramped fluence beam until failure occurs. The ensemble of individual thresholds generated is used to determine the cumulative failure probability curve for the sample. The R/1 test represents the maximum degree of laser conditioning attainable on a sample.

The linearly polarized laser operated at 1064 nm at 10 Hz with pulse duration of 10 ns (FWHM), and the spatial profile on target was gaussian with a diameter of 1 mm (FW@$1/e^2$). At this pulse length, the maximum fluence in the NIF beam (1.24:1 pk:ave) is 31.2 using $t^{0.5}$ scaling.

2. TEST RESULTS

2.1 S/1 tests on unannealed samples

S/1 tests were performed on each sample prior to thermal annealing to establish baseline damage curves and examine changes in damage with position in the boule (or growth history). The results of these tests are shown in Figure 2. Fluence measurement precision was ± 10 percent.

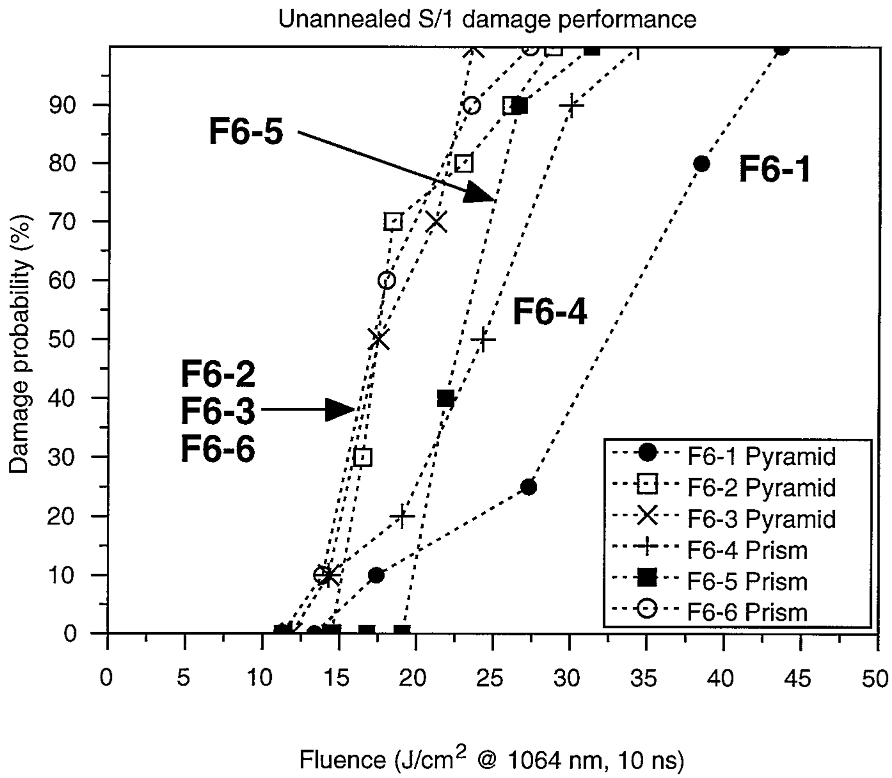

Figure 2. S/1 test results for unannealed F6 doubler samples. The last grown pyramid sample, F6-1 has the highest damage performance. Otherwise, no systematic correlation to sample location within the boule is apparent.

As shown in the figure, the last grown pyramidal sample F6-1 has higher damage resistance than the other samples. This possibly could be attributed to last grown material having higher purity than early or middle growth material (due to solution cleaning by impurity uptake into the prism sector), but additional testing on other boules is required to determine if this is a systematic trend. The other pyramidal samples, F6-2 and F6-3 have lower damage curves and are either comparable to or lower than the 3 prismatic samples (F6-4 through F6-6) which do not show any correlation to growth time. Based on these curves all the samples except F6-1 would suffer substantial bulk damage on a full fluence NIF shot and therefore cannot be considered acceptable. The unannealed performance of F6-1 would be considered marginal for NIF operation where the average and maximum fluence at the doubler are expected to be ~13.8 J/cm^2 and 17.1 J/cm^2 at 3 ns respectively. This corresponds to fluences of 25.2 J/cm^2 and 31.2 J/cm^2 at 10 ns using $t^{0.5}$ scaling.

2.2. S/1 test results after thermal annealing

The samples were annealed at 160°C for seven days under ambient atmospheric conditions (~50% relative humidity). This matches the annealing cycle of previously tested KDP crystals and was originally chosen based on experiments[3] showing that bulk scatter was minimized for these parameters. The results of post-anneal S/1 tests are shown in Figure 3.

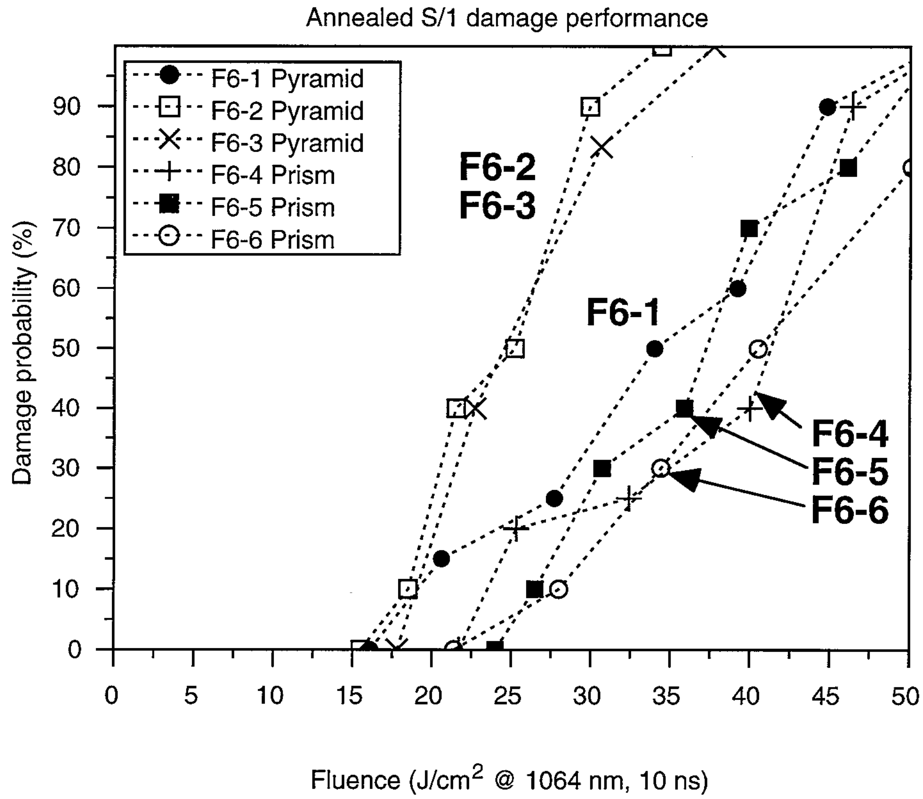

Figure 3. Results of S/1 damage tests on post-annealed samples. The prismatic sector samples showed the greatest effect with 50% damage fluences increasing from 1.6X to 2.4X over the unannealed samples. The pyramidal samples showed only a maximum increase of 1.4X.

Thermal annealing resulted in dramatic increases in the damage performance of the prismatic crystals with improvement ranging from 1.6X for sample F6-5 to 2.4X for F6-6. The degree of conditioning was determined by the change in the fluence at 50% damage probability. Thermal annealing was less effective for the pyramidal samples. Sample F6-2 and F6-3 increased from ~16 to 24 J/cm^2 while F6-1 increased from 33 to 34 J/cm^2. The average degree of conditioning for the pyramidal samples was 1.4X.

2.3. S/1 test results with in-situ second harmonic generation

After the samples had been thermal annealed and damage tested, the S/1 tests were repeated, this time with in-situ second harmonic generation (SHG). In all previous tests the samples were oriented so that the incident electric field vector was polarized parallel to the extraordinary (e) axis of the crystal, so that no doubling could take place. For the SHG tests, either the sample or the laser polarization was rotated to the ordinary axis (o) of the crystal and SHG occurred. A superpolished, 3 degree, fused silica wedge was installed downstream from the test crystal to sample the combined 1ω/2ω beam. The first surface Fresnel reflection was directed to a dichroic beam splitter for residual 1ω removal, after which the 2ω energy was measured. The conversion efficiency was maximized at non-damaging fluences by adjusting the polarization of the incident 1ω beam and angle tuning the crystal. To determine the expected degree of second harmonic generation, the conversion process was computer modeled using LLNL frequency conversion codes, taking into account the beam geometry, temporal profile, crystal thickness and lack of AR coatings.

The S/1 tests were performed on all the samples after checks on diagnostics were made to ensure that the 532-nm light would not lead to false positives. In addition, an R/1 test was made on sample F6-6 (prism). The results of these S/1 tests are shown in Figure 4. The figure also shows the predicted second-harmonic conversion efficiency from computer modeling as well as the measured efficiency from sample F6-6.

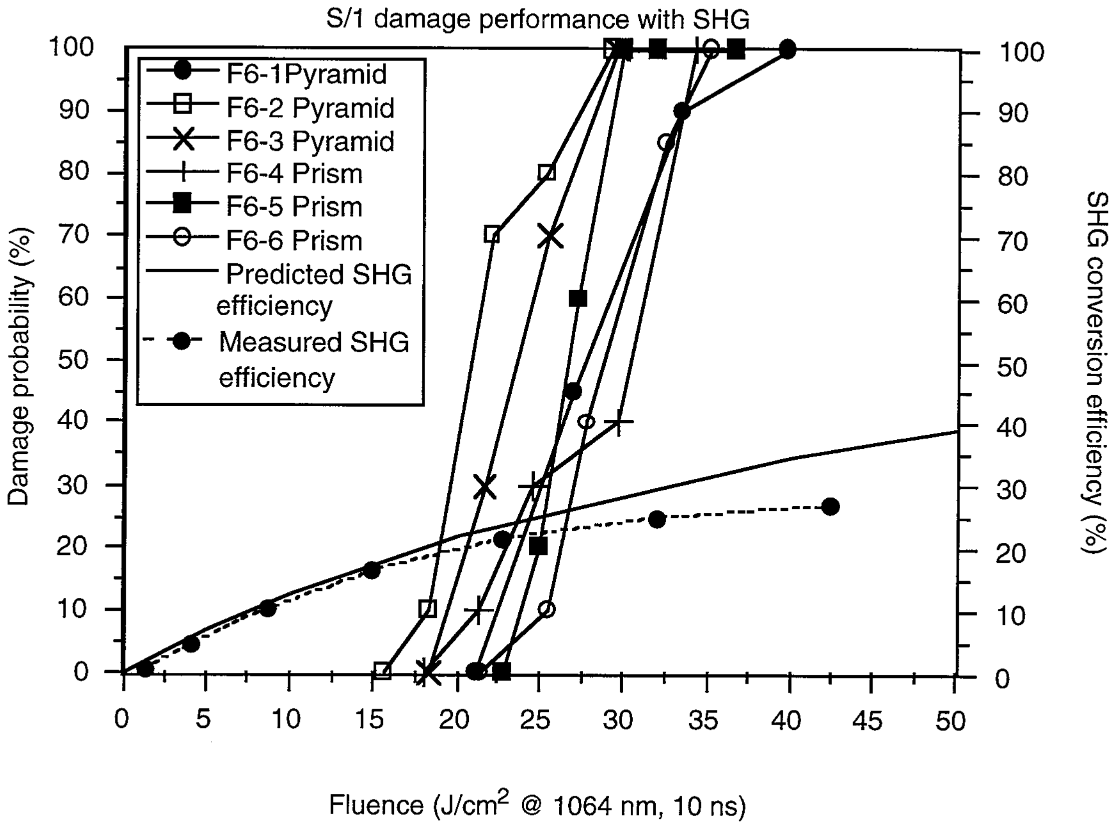

Figure 4. Results of S/1 damage tests with in-situ SHG. The damage performance is reduced by an average of 20% from the non-SHG case.

Comparison of the SHG S/1 data to the post-annealed-1ω-only tests (Figure 3) indicates that the 50% damage fluence has been reduced by an average of 20%. The second harmonic generation curve shown for sample F6-6 represents the highest efficiency measured for all the samples and compares very well with the predicted response. The other samples typically showed a few percent less conversion efficiency that was attributed to angle detuning. The roll-off in measured SHG at fluences above 20 J/cm^2 was possibly due to the occurrence of damage and/or pump depletion and was observed for all samples.

To ensure that the downward fluence shift in the damage-probability curves with the presence of SHG was actually due to the conversion process, the SHG S/1 test was repeated on samples F6-5 and F6-6 but with the crystals angle detuned to the second sidelobe minimum of the angle-tuning curve. This preserved the o-polarization of the incident beam while suppressing the SHG process. In both samples tested, the S/1 damage curves were essentially identical to their e-polarization (1ω only) counterparts. As an example, the tests for sample F6-5 (prism) are shown in Figure 5.

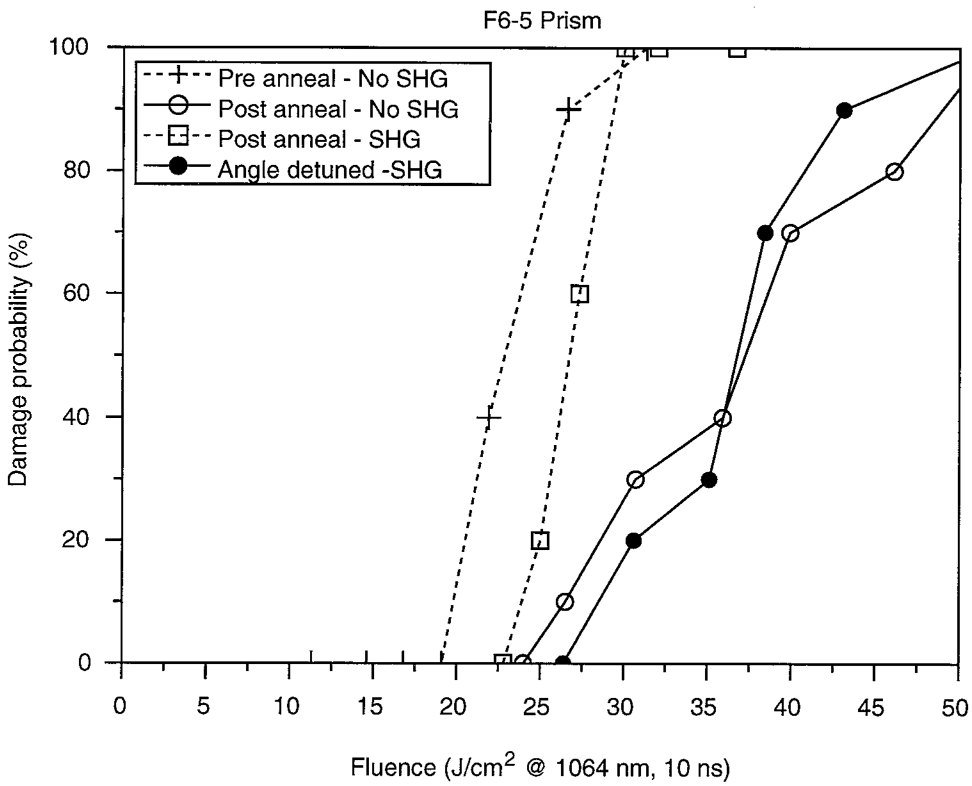

Figure 5. S/1 test results for sample F6-5 (prism) showing sample behavior before and after annealing at 1ω only (e-polarization) and after annealing with 2ω generation and 2ω suppressed by angle detuning (o-polarization). Angle detuning returns the curve to its e-polarization, 1ω only result.

Table 1 shows a compilation of 50% damage probability fluences for unannealed, annealed and annealed with SHG for all samples tested.

Table 1. Compilation of unconditioned damage data for F6 samples.

Sample	Sector	Growth Temp (°C)	Growth Day	Unannealed (J/cm^2)	Annealed (J/cm^2)	Annealed with SHG (J/cm^2)
F6-1	Pyramid	48	40	32	33	26
F6-2	Pyramid	63	30	17	23	18
F6-3	Pyramid	72	14	17	23	23
F6-4	Prism	71	20	23	40	30
F6-5	Prism	60	33	21	37	36
F6-6	Prism	25	48	17	40	28

2.4 R/1 test results on sample F6-6

In addition to the S/1 tests, sample F6-6 also received R/1 tests at each stage of the crystal evaluations. Because of the multitude of tests performed on this sample, the R/1 tests were limited to 50 sites each. The results of these tests are shown in Figure 6.

In the unannealed case, laser conditioning is responsible for raising the 50% failure fluence by a factor of 2.1 over the unconditioned, S/1 case. After thermal annealing, the increase due to laser conditioning is only 1.5X over the annealed S/1 result, but the combined increase over the unannealed S/1 result is 3.5X. For the annealed case, the presence of second harmonic generation reduces the S/1 values to 0.7X and the R/1 values by 0.6X of their 1ω only values. The change between all test cases is given in Table 2.

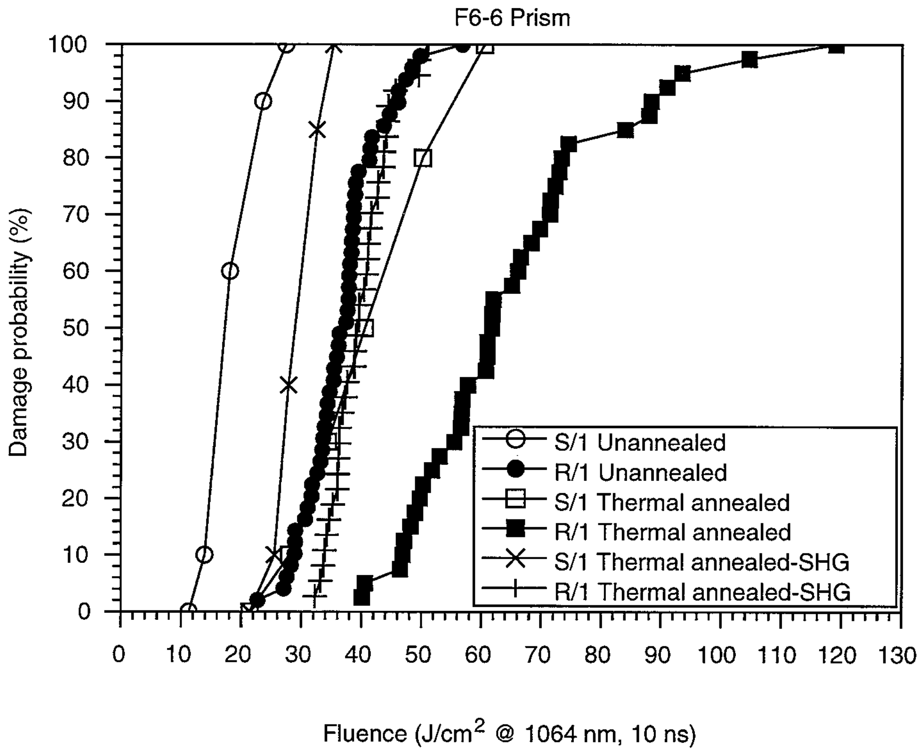

Figure 6. Results of R/1 testing for sample F6-6 (late growth prism). The effect of thermal annealing is significant in raising the damage performance, but the presence of SHG reduces the annealed curve almost to the unannealed, 1ω only result.

Table 2. Change in 50% damage probability fluence due to thermal annealing, laser conditioning and second harmonic generation for sample F6-6.

	S/1 unannealed (17.5 J/cm^2)	S/1 annealed (40.5 J/cm^2)	S/1 SHG (29.0 J/cm^2)	R/1 unannealed (36.5 J/cm^2)	R/1 annealed (61.5 J/cm^2)	R/1 SHG (39.0 J/cm^2)
S/1 unannealed	1.0	2.3	1.7	2.1	3.5	2.2
S/1 annealed	0.4	1.0	0.7	0.9	1.5	1.0
S/1 SHG	0.6	1.4	1.0	1.3	2.1	1.3
R/1 unannealed	0.5	1.1	0.8	1.0	1.7	1.1
R/1 annealed	0.3	0.7	0.5	0.6	1.0	0.6
R/1 SHG	0.4	1.0	0.7	0.9	1.6	1.0

The 50% failure fluence is given in parenthesis across the top row. The change is determined by dividing the row fluence by the column fluence for the appropriate element in the table. Transpose elements are their reciprocals. I.e. $x_{ij} = 1/x_{ji}$.

2.5 Impurity analysis of samples

Following damage testing, the samples were analyzed for cationic impurity concentration using ICP-MS techniques. Ionic impurities of aluminum, silicon, sulfur, titanium, iron, strontium, zirconium, antimony and barium were detected in the prismatic samples while only barium and strontium were detected in the pyramidal samples. The concentrations of the ionic impurities are plotted in Figure 7 along with the temperature profile of the growth solution. The data shows that barium, strontium and titanium concentrations drop during growth. This is due to uptake of these impurities by the prism from the growth solution. On the other hand, aluminum, silicon, zirconium and iron concentrations increase over the course of the growth run. This is attributable to leaching of these impurities from the walls of the glass tank and uptake primarily by the prism sector.

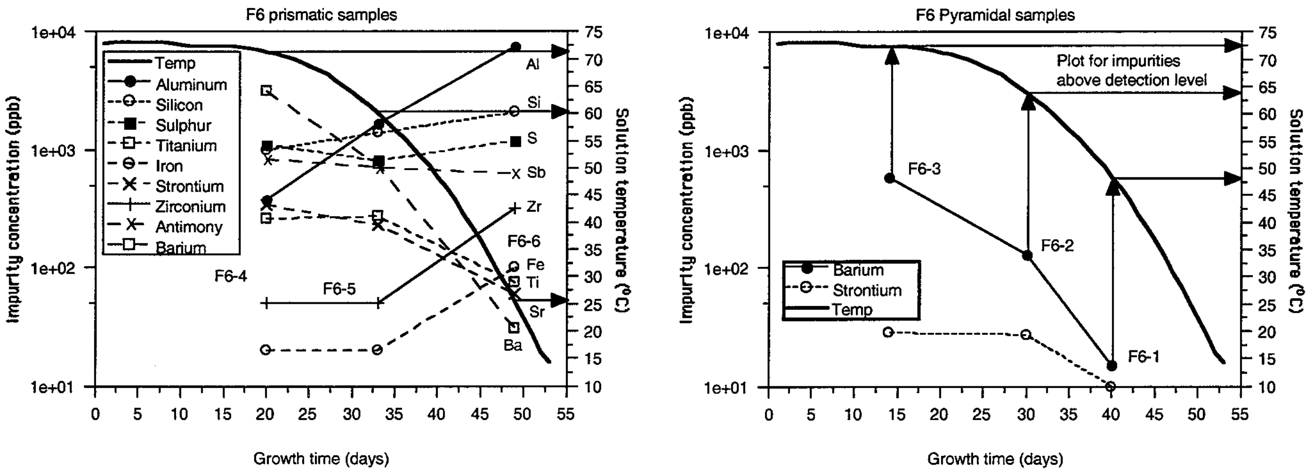

Figure 7. The evolution of ionic impurity concentration for prism and pyramidal samples as a function of growth time and solution temperature.

3. DISCUSSION OF RESULTS

3.1 The effect of impurities and growth temperature on damage

Examination of the 50% damage probability table (Table 1) and Figure 7 allows a number of comments to be made. First, the most damage resistant sample for unannealed tests was F6-1. This was the last grown pyramidal sample where impurities were at the lowest levels in the crystal. The solution temperature was approximately 48°C when this sample was grown. This temperature is at the threshold for producing highly damage resistant material[8], so it is not unexpected that this crystal would be best among the sample set. Second, the prismatic samples exhibited the substantially higher increases in damage resistance due to thermal annealing than the pyramidal material. The largest increase was exhibited by sample F6-6 where aluminum, silicon, iron and zirconium concentrations were at their maximum. The growth temperature for this sample was approximately 25°C. This was the only sample grown at a temperature below 45°C where high damage resistance has been observed on DKDP at 3ω [8]. Given that the higher purity pyramid samples did not exhibit substantial increases in damage resistance while the prismatic samples did, it appears that some level of impurities are needed to achieve maximum increases from thermal annealing. Indeed, in [8] we observed that growth temperature seemed to be the most significant factor in increasing the damage resistance of DKDP at 3ω despite the fact that some of the samples contained substantial levels of iron and aluminum. Due to the complicated nature of the impurity incorporation process, it is not possible to determine which impurities are needed based solely on the data from F6 samples. However, this question is currently being intensively investigated.

3.2. SHG performance on NIF

Prior to discussing the implications of these results for NIF SHG performance a few comments are in order. In many ways the damage situation for 1ω is analogous to that for 3ω. First, the pulse length scaling law for bulk damage at 1ω is unknown, although the 3ω pulse scaling law appears to go as $t^{0.35}$ [7]. The 10-ns time scale of the 1ω laser pulse allows the built up heat from a damage event to diffuse in KDP so the $t^{0.5}$ scaling associated with 1-dimensional heat flow should be reasonable whether the damage initiator is a nanometer scale foreign absorber or intrinsic crystal defects. Next, the obscuration and scattering behavior of pinpoint damage has not been characterized, therefore it is not known which damage curve corresponds to the 0.1% obscuration specification for NIF crystals. In addition, there is no data on 1ω bulk damage in large beam environments (e.g. OSL, Slablab) where damage evolution as a function of fluence, pulse duration and number of shots has been measured. It is probable that damage increases steeply with fluence as in the 3ω case[4,5,7]. Attempts at modeling 1ω and 3ω damage curves using Poisson statistics with exponential evolution[4] have shown that 1ω pinpoint density does not increase as rapidly as in the 3ω case. Finally, small beam experiments have shown that KDP can withstand substantially higher fluences at 1ω than at 3ω, so it is reasonable to assume that 1ω damage might be more benign. These considerations have led us to conclude (by analogy to 3ω that a damage curve that crosses the NIF redline fluence (33.3 J/cm^2 at 10 ns using $t^{0.5}$ scaling) at approximately 20% failure probability will be adequate for use on NIF. Bearing this in mind it is now possible to interpret the F6 test data relative to NIF operation.

Considering 1ω operation alone, the unconditioned, unannealed F6 samples would not be adequate for NIF SHG operation at full fluence. Reducing NIF operating fluences by 40% (i.e. operating at average 3ω, 3 ns fluences of 5 J/cm^2) still does not qualify this material without annealing. In contrast, thermal annealing increases the damage resistance to the point where the boule would qualify for operation at 60 percent of the NIF maximum, but the boule would still not qualify for full fluence shots.

The increase in S/1 damage probability with SHG disqualifies the annealed boule from even low fluence shots without laser conditioning. Considering that less than 30% conversion efficiency is attained in the small beam geometry of these experiments, the reduction in damage performance is likely to be worse on NIF where the efficiencies are expected to be at least 60%. Therefore, it appears that the only way to qualify this boule, or similar material for full fluence NIF SHG operations is through a combination of thermal annealing and laser conditioning. The 50% failure probability fluence cannot be reduced by more than 15% by SHG (at 60% conversion efficiency) and still meet the NIF obscuration requirement.

Purchase and construction of a dedicated 1ω conditioning system to laser condition NIF doublers is anticipated to cost in the vicinity of $0.5 to 1 million. A scanning system based on the design of table-top conditioning systems for laser glass slabs can be constructed in a short time.

However, due to the recent discovery of the 1.5X-2.0X difference between z-plate and THG cut crystals at 3ω (THG crystals exhibit higher damage probability) it is highly likely that a 3ω laser conditioning system will be built. The requirement to scan a single NIF tripler in one day requires the average power which cannot be delivered with table-top Nd:YAG systems. Recent studies[6] have shown that substantial damage improvement at 3ω can be attained using excimer lasers at 308 nm or 351 nm. Industrial grade lasers of this type do possess the high average power needed to meet the scan time requirement. During the preparation of this report, we found that 3ω irradiation dramatically improves damage performance at 1ωas shown in Figure 8, so a stand-alone 1ω conditioning system will not be needed. In this experiment we raster scanned an x-cut sample from rapid growth DKDP boule CD35 (see [2] for details about this crystal) at a fluence of 5 J/cm^2 using the Zeus laser at 355 nm. Subsequently the virgin and raster scanned areas were damage tested at 1064 nm. As shown in the figure, the untreated area had a 50% damage fluence of approximately 20 J/cm^2. In contrast, we were unable to obtain bulk damage probabilities greater than 10 percent for *any* fluence tested in the 5 J/cm^2 rastered area up to 110 J/cm^2 at 10 ns.

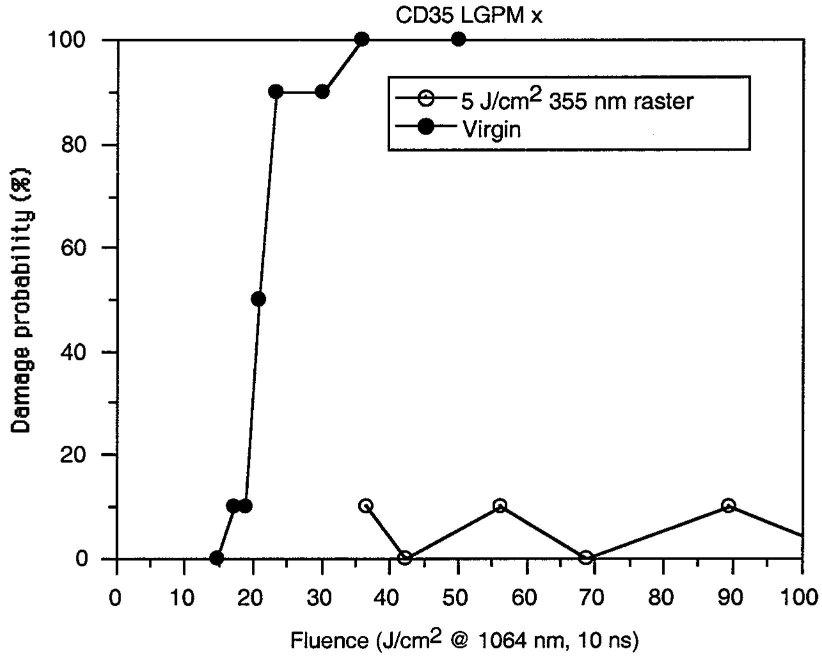

Figure 8. The increase in 1ω damage resistance due to raster scanning at 355 nm with 5 J/cm^2 beam fluence. Damage probabilities greater than 10 percent for the rastered area were not observed despite fluences exceeding 100 J/cm^2 at 10 ns.

3.3 Summary

The tests performed here have addressed 1ω bulk damage issues for current state-of-the-art rapid growth KDP for use on NIF. S/1 tests of unannealed material have shown that there is variation within the boule that may be related to impurities in the prismatic sector. Thermal annealing at 160°C for 7 days has been shown to increase the damage performance of the prismatic material by up to 2.4X while leaving the pyramidal material almost unaffected.

In-situ second harmonic generation experiments have shown that for conversion efficiencies between 25 and 30 percent, the damage performance will be reduced by 20 percent for unconditioned, S/1 tests and by 40 percent for laser conditioned material. While results on these samples indicate that some type of conditioning is needed to meet NIF obscuration requirements, recent raster scanning experiments have shown that only modest 3ω fluences (5 J/cm^2) are required to yield doublers which will not be damaged by NIF fluences.

ACKNOWLEDGMENTS

This work was performed under the auspices of the U.S. Department of Energy by the University of California Lawrence Livermore National Laboratory under contract No. W-7405-Eng-48.

REFERENCES

1. M. Runkel and S. Weinzapfel, "Results of recent 1ω automated damage testing on KDP," NIF-6731, LLNL internal memo, April 1998
2. M. Runkel and A. Burnham, "Differences in bulk damage probability distributions between tripler and z-cuts of KDP and DKDP at 355 nm," SPIE Proceedings for this symposium, October 2000
3. B. Woods, M. Runkel, M. Yan, J.J. DeYoreo, M. Kozlowski, "Optical scatter as a diagnostic tool for studying bulk defects which cause laser damage in conventional and rapid growth KDP and DKDP," in Optical Scattering in Optics, Semiconductors, and Computer Disk Industries, SPIE Proceedings, Volume **2541**, J.C. Stover, ed. SPIE, Bellingham, WA, 1995

4. M. Runkel, J. DeYoreo, W. Sell, D. Milam, "Laser conditioning study of KDP on the Optical Sciences Laser using large area beams," SPIE Proceedings, Volume 3244, pages 51-63, 1997
5. M. Runkel and R. Sharp, "Modeling KDP damage curves for the prediction of large area damage performance," SPIE Proceedings, Volume 3902, pages 436-447, 1999
6. M. Staggs, M. Runkel, M. Yan, "Laser conditioning of KDP and DKDP crystals using and excimer laser," SPIE Proceedings for this symposium, October 2000
7. M. Runkel, A. Burnham, W. Sell, D. Milam, M. Feit, A. Rubenchik, "The results of pulse-scaling experiments on rapid growth DKDP triplers using the Optical Sciences Laser at 351 nm," SPIE Proceedings of this symposium, October 2000
8. A. Burnham, M. Runkel, R. Hawley-Fedder, L. Carman, R. Torres, P. Whitman, "Low temperature growth of DKDP for improving laser-induced damage at 350 nm," SPIE Proceedings of this symposium, October 2000